SEMARAK ILMU PUBLISHING

CFD Letters

Journal homepage:
https://semarakilmu.com.my/journals/index.php/CFD_Letters/index
ISSN: 2180-1363

Aerodynamic Characteristics of Overtaking Bus under Crosswind: CFD Investigation

Aan Yudianto[1,*], Herminarto Sofyan[1], Gunadi[1], Naufal Annas Fauzi[2]

[1] Automotive Design Laboratory, Department of Automotive Engineering Education, Faculty of Engineering, Universitas Negeri Yogyakarta, Yogyakarta, Indonesia
[2] Department of Transport Eksploatacja i Mechatronika Samochodów, Politechnika Krakowska, Krakowska, Poland

ARTICLE INFO

Article history:
Received 25 May 2022
Received in revised form 8 July 2022
Accepted 23 July 2022
Available online 31 August 2022

Keywords:
Aerodynamics; bus; CFD; crosswind; overtaking; simulation; yaw

ABSTRACT

The presence of other vehicles, travelling together on the road, highly contributes to the condition on the realistic air flow direction. The position alteration of other vehicles generates different airflow direction which is unpredictable experienced by the vehicle under investigation. It considerably affects the stability of a vehicle having large size of the body. The purpose of the study was to investigate the aerodynamic response of a detailed bus model in overtaking process with the interference of crosswind. Fluidic simulation was performed to investigate the air flow behavior imposed on the bus by means of Computational Fluid Dynamics (CFD) analysis. A scaled bus model was used in the simulation with the different positions representing the buses during the overtaking process. The coefficient X/L was introduced to realize the vehicle position during the overtaking process. The results discussed the alteration of drag force coefficient, lift force coefficient, side force coefficient, during the position on overtaking process. The resulting turbulence kinetic energy around the bus was also discussed by comparing the case without crosswind and when the yaw angle was 30°. The most prominent aerodynamic forces alteration occurs when the overtaking process was at X/L=1. Further explanation about the pressure coefficient at the surface of the bus and the area around the vehicle was investigated at this position. The accuracy of numerical results calculation was verified by comparing the result of simulation and experimental testing of Cd and Cl with the percentage of deviation 0.37% and 2.90% respectively.

1. Introduction

The airflow over a road vehicle generates a complex flow field resulted from the varying body shape of the vehicles running on the road and driving conditions including crosswind. The flow becomes more intricate when two road vehicles are in the overtaking process. As a result, the aerodynamic forces imposed on the vehicles vary as the position of the vehicles during the overtaking process changes which affects the vehicle's stability and safety [1-6]. Moreover, a crosswind causes problems for the vehicle's motion and drivability since there are additional lateral air velocity

* *Corresponding author.*
E-mail address: aan.yudianto@uny.ac.id (Aan Yudianto)

https://doi.org/10.37934/cfdl.14.8.2032

components [7]. This issue becomes more severe for a large vehicle such as an intercity bus [8-10].

Some studies to investigate the aerodynamic behavior on different driving conditions of large vehicles such as a bus, truck, and trailer have been conducted to study, optimize and experimentally test the aerodynamic characteristics of the vehicle [11-15]. There are also numerous existing numerical and experimental research to investigate the effect of crosswind on a double-deck bus, moving vehicle under crosswind, vulnerability assessment of crosswind and even on passenger trains [16-23]. Their results indicate that generally the side force coefficient of the vehicle due to the presence of crosswind increases as the lateral velocity component due to crosswind elevates. Crosswind itself is not the only factor increasing the uneven airflow condition. However, the overtaking process of vehicles also plays an essential contribution to the instability of the vehicle. Some scholars investigate overtaking process either in simulation on by experimental testing [8,24-26]. Some other researchers also examine the combination between overtaking processes along with the presence of crosswind [27,28]. The investigation includes the effects of aerodynamic force coefficients and the visualization of the flow field around the vehicle.

Most of the mentioned studies were mainly concerned about the effect of crosswind on the aerodynamic characteristics of a simple vehicle model. However, the effects of detailed bus model on the aerodynamic characteristics with the case of overtaking position with another bus by considering asymmetric flow condition is not fully covered and requires a further investigation. This study focused on the investigation of both the overtaking process along with the absence and the presence of crosswind on a detailed intercity bus model with the proposed three-dimensional numerical simulation method. Both aerodynamic characteristics of overtaking and overtaken bus including aerodynamic forces coefficient, pressure coefficient, and resulting turbulence kinetic energy are numerically and visually analyzed.

2. Methodology

2.1 Bus Geometry Definition

The study used a 1:10 scaled bus model with the dimension is depicted in Figure 1. The length (L) of the bus was 1243 mm, the width (W) was 267 mm, and the overall height (H) was 333 mm. The model used a wheel radius (R) of 50 mm. The assumption of a contact point between the tire and the road was flat due to the elasticity of the tire and the weight of the bus as shown in Detail A in Figure 1. The distance between the front and rear wheel was 627 mm followed by a diffuser with an angle of 5 degrees towards the rear of the bus model. The intersection of the front shield and the upper part of the bus is considered a 9-degree angle slope. The upper part also modeled a compartment where usually an air conditioner equipment was located. The model was also equipped with a pair of mirrors with the dimension was depicted in Figure 1. The door handle, however, was eliminated for the sake of simplicity but keeping the calculation accuracy and the lower part of the bus model was also assumed as flat ignoring the shape of small parts at the underbody. The same assumption applied at the side part of the model disregarding the outer shape of the bus windows.

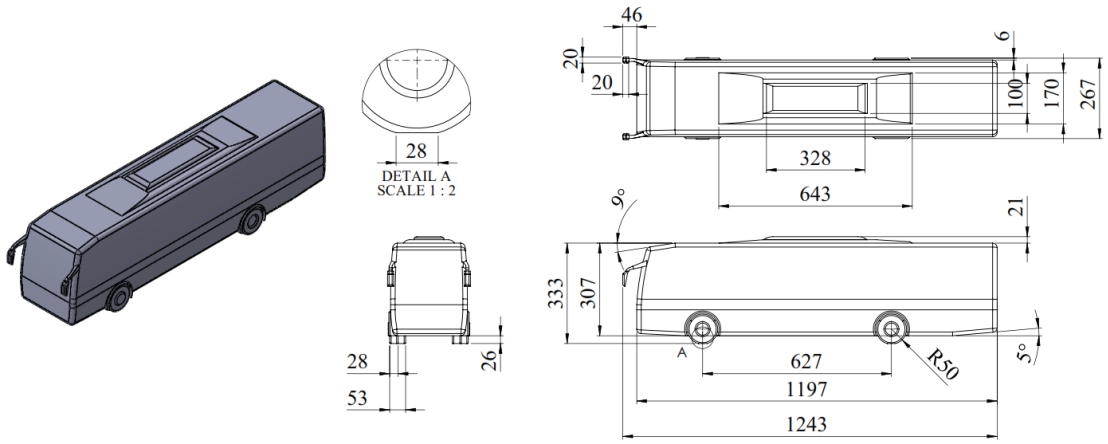

Fig. 1. A detailed intercity bus model (dimensions in mm)

2.2 Computational Domain

A cuboid periphery of the computational domain was employed with the overall length 10L, overall width 15W, and overall height 5H. The bus was overtaking on the right side of the overtaken bus so that bus2 represented the overtaking bus and bus1 was the overtaken one. The computational domain utilized two inlet faces and two outlet faces namely inlet1, inlet2, outlet1, and outlet2 as explained in Figure 2. The lower part of the cuboid surface was set as a slip wall represents the moving road surface. The distance between the inlet 1 and the front part of the bus varied depending on the overtaking position yet keeping 4W as the distance between the inlet2 face and the left side of the bus1 model and 8W as the distance between bus2 model and the outlet2 face of the computational domain.

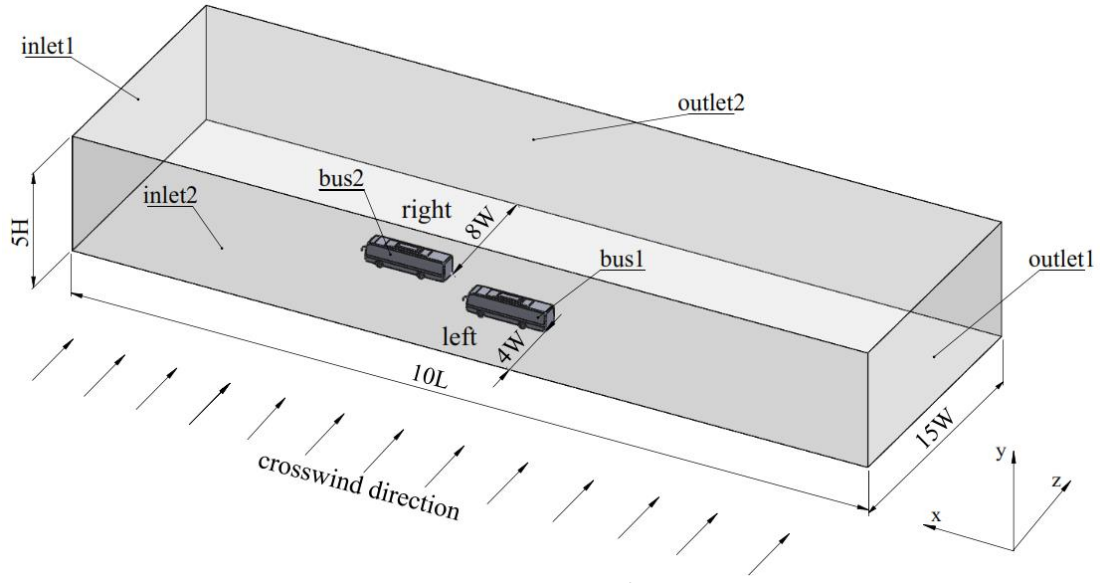

Fig. 2. Computational domain of the overtaking bus

2.3 Mesh Technique

The mesh generation adopted a hybrid mesh method, utilizing poly-hexcore volume mesh. The smooth transition with three layers was set up at boundary layer settings on fluid walls. To ensure the quality of the calculation, the minimum size of the element was determined at 0.011 m and the

maximum size was 0.30 m with a 1.2 growth rate. Moreover, to efficiently capture the complex shape of the bus model and effectively create the mesh, the local sizing around the area of Bus1 and Bus2 was determined by setting the local min size also 0.01. This setting allows the resulting mesh to generate the mesh results as closely similar as possible to the original model in reality as shown in Figure 3. The resulting mesh produces 812,657 nodes, 6,415 edges and 1,261,389 faces. It can be observed that the generated mesh already represented the real shape of the model and high potential to generate accurate calculation results.

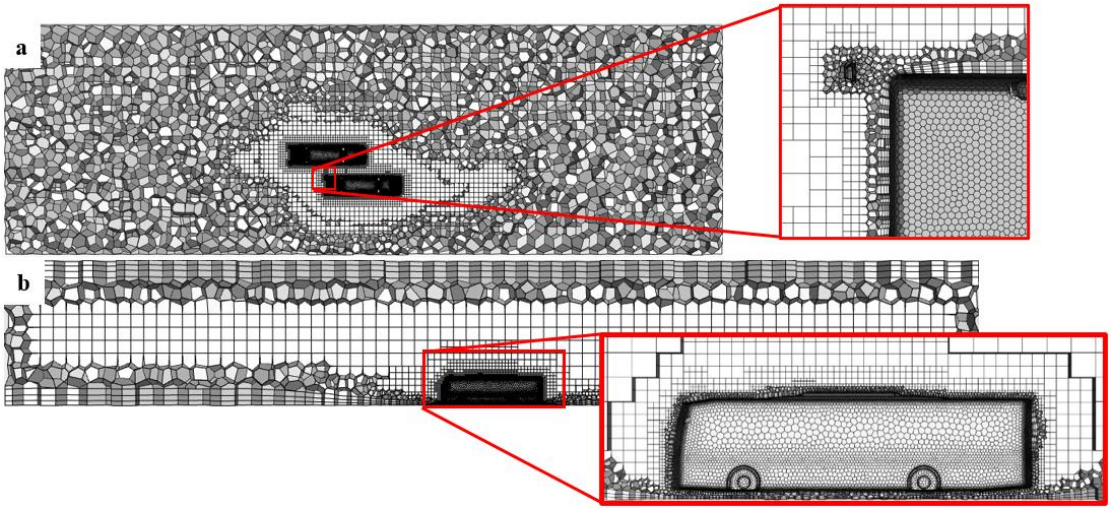

Fig. 3. Mesh strategy during the overtaking position

2.4 Bus Position and Airflow Direction

The typical velocity and natural direction of crosswind vary irregularly over time. However, it was assumed that the velocity and direction of crosswind were constant in every overtaking position and the direction was perpendicular to the bus motion. Instead of keeping two buses in motion, the simulation kept the bus position unchanged and set the velocity of the incoming flow and the crosswind to flow over the bus model. The velocity of incoming flow 10 m/s (v_{if}) flowed through the bus model in the -x direction. To simulate the bus2 that was overtaking another bus, the surface of bus2 was set having relative velocity (v_{rel}) 3 m/s at the direction of +x. By doing so, this means that bus1 run 10 m/s and was overtaken by bus2 having a velocity of 13 m/s. The crosswind velocity (v_{cw}) flowed from the side of the bus perpendicular to the bus motion with a direction of +z. Therefore, a yaw angle (α) was produced and defined as the angle between the centerline of the bus and the direction of the resulting velocity (v_{res}). Since there were three cases applied to the simulation in this study, there were also three different crosswind velocities for different yaw angles. The velocity of incoming flow was kept as a constant value of 10 m/s and there are three different yaw angles at $\alpha = 10°$, $\alpha = 20°$, and $\alpha = 30°$, with the crosswind velocity was respectively set at 1.76 m/s, 3.64 m/s, and 5.77 m/s.

The resultant velocity (v_{res}) was defined as the vehicle's velocity relative to the direction of the air stream flowing through the Bus1 as follows.

$$v_{res} = \sqrt{v_{if}^2 + v_{cw}^2} \tag{1}$$

$$\alpha = arc\tan\left(\frac{v_{cw}}{v_{if}}\right) \quad (2)$$

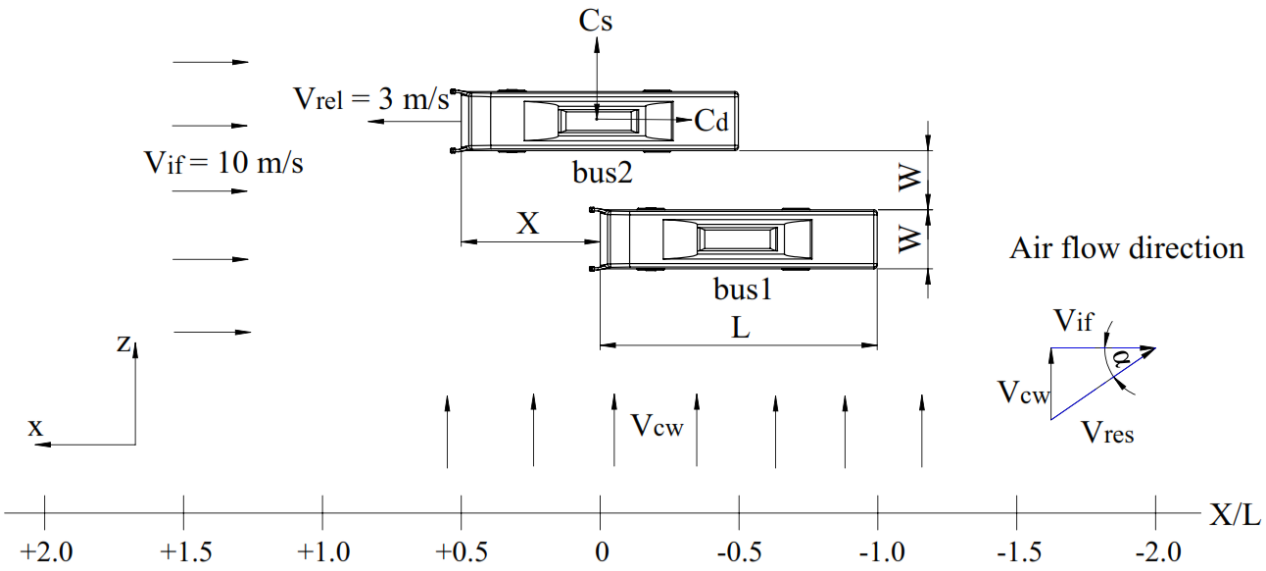

Fig. 4. Bus position and wind direction

Therefore, it can be noted that the vector summation of v_{if}, v_{rel}, and v_{cw} generates the resultant velocity (v_{res}) for Bus2 as follows.

$$v_{res} = \sqrt{\left(v_{if} + (-v_{rel})\right)^2 + v_{cw}^2} \quad (3)$$

Furthermore, the equation for the yaw angle of Bus2 is:

$$\alpha = arc\tan\left(\frac{v_{cw}}{v_{if}+(-v_r)}\right) \quad (4)$$

At this point, it is clear that there is a difference between the yaw angle of Bus1 and Bus2. Therefore, the yaw angle of Bus1 was used as the reference yaw angle of all simulations and results in the discussion. The X/L coefficient was introduced to represent the relative displacement between two buses during the process of overtaking. The X represents the longitudinal distance between Bus1 and Bus2 measured from the front part of the bus. The L value is the length of the bus model. In this study, the corresponding distance during the overtaking process varied from X/L = -2 to X/L = 2. The following discussion divides the X/L in every 0.5.

2.5 Operating and Boundary Conditions

The SST k-ω turbulence model was used in the simulation. The fluid was set to constant density air with the value of 1.225 kg/m3 with the temperature 288.16°K. This indicates that the air pressure was 1.01325x10^5 Pa. The viscosity was 1.7894x10^{-5} kg/m-s. Table 1 shows the setting of boundary conditions.

Table 1
Settings of boundary conditions in the simulation

No	Boundary condition	Settings
1	Inlet1	Velocity-inlet: $v_x = v_{if}$, $v_y = v_{cw}$, $v_z = 0$
2	Inlet2	Velocity-inlet: $v_x = v_{if}$, $v_y = v_{cw}$, $v_z = 0$
3	Outlet1	Pressure-outlet: atmospheric pressure
4	Outlet2	Pressure-outlet: atmospheric pressure
5	Top	Slip wall
6	Road surface	Slip wall
7	Bus surface	No-slip wall

2.6 Aerodynamic Coefficient Definition

The process of a bus overtaking another bus involved aerodynamic forces and pressure that were expressed as non-dimensional coefficients. Three force coefficients namely drag force coefficient (C_D), lift force coefficient (C_L), and side force coefficient (C_S) also one pressure coefficient (C_p) are expressed as follows:

$$C_D = \frac{F_D}{\frac{1}{2}\rho v_{res}^2 A} \tag{5}$$

$$C_S = \frac{F_S}{\frac{1}{2}\rho v_{res}^2 A} \tag{6}$$

$$C_L = \frac{F_L}{\frac{1}{2}\rho v_{res}^2 A} \tag{7}$$

$$C_p = \frac{p - p_{if}}{\frac{1}{2}\rho v_{if}^2} \tag{8}$$

where F_D is the drag force, F_S is side force, and F_L is lift force. The ρ represents the density of the air flowing through the bus model. A denotes the projection area of the bus. v_{res} indicates the resultant velocity. The resultant velocity of Bus1 depends on the vector resultants of v_{if} and v_{cw}, while Bus1 was determined by the resultant vector of v_{if}, v_{rel} and v_{cw}. The pressure around the bus was also expressed by a dimensionless coefficient. p denotes as static pressure in which the area is evaluated, p_{if} is the static pressure in the free stream, ρ is the density of the air and v_{if} is the incoming flow velocity.

3. Results

The discussion of the results focusing on aerodynamic force coefficients, turbulence kinetic energy, flow streamlines, and pressure coefficient are investigated as follows.

3.1 Effect on Cd, Cl, and Cs

Figure 5 shows the effect of bus overtaking position on the performance of aerodynamic forces coefficient on overtaking and overtaken bus at different yaw angles. It can be noted that with the higher magnitude of yaw angle, the value of nearly all aerodynamic coefficients elevates, especially the side force coefficient. This result matches the previous studies by Zhang *et al.,* [15], Dorigatti *et*

al., [21], and Suzuki *et al.,* [29]. As it is compared in Figure 5(a) and Figure 5(b), the drag coefficient of two buses hovers at the value of 0.42 with the absence of crosswind. However, the value of C_D elevates as the yaw angle increases. As for Bus1, the highest value of C_D occurs when the yaw angle is $30°$ at the position of X/L between 0 and 0.5. It then goes down to the value of around 0.82 when X/L equals to 1. Other values of C_D remains unchanged for lower yaw angle ($\leq 20°$). Striking results can be observed for Bus2. The drag coefficient of bus 2 relatively similar between 0.43 – 0.65 at all yaw angle from X/L = -2 to X/L = 0.5. It then jumps to the value around 1.2 when X/L =1 at $30°$ yaw angle. The following results of C_D go down to the value 0.8.

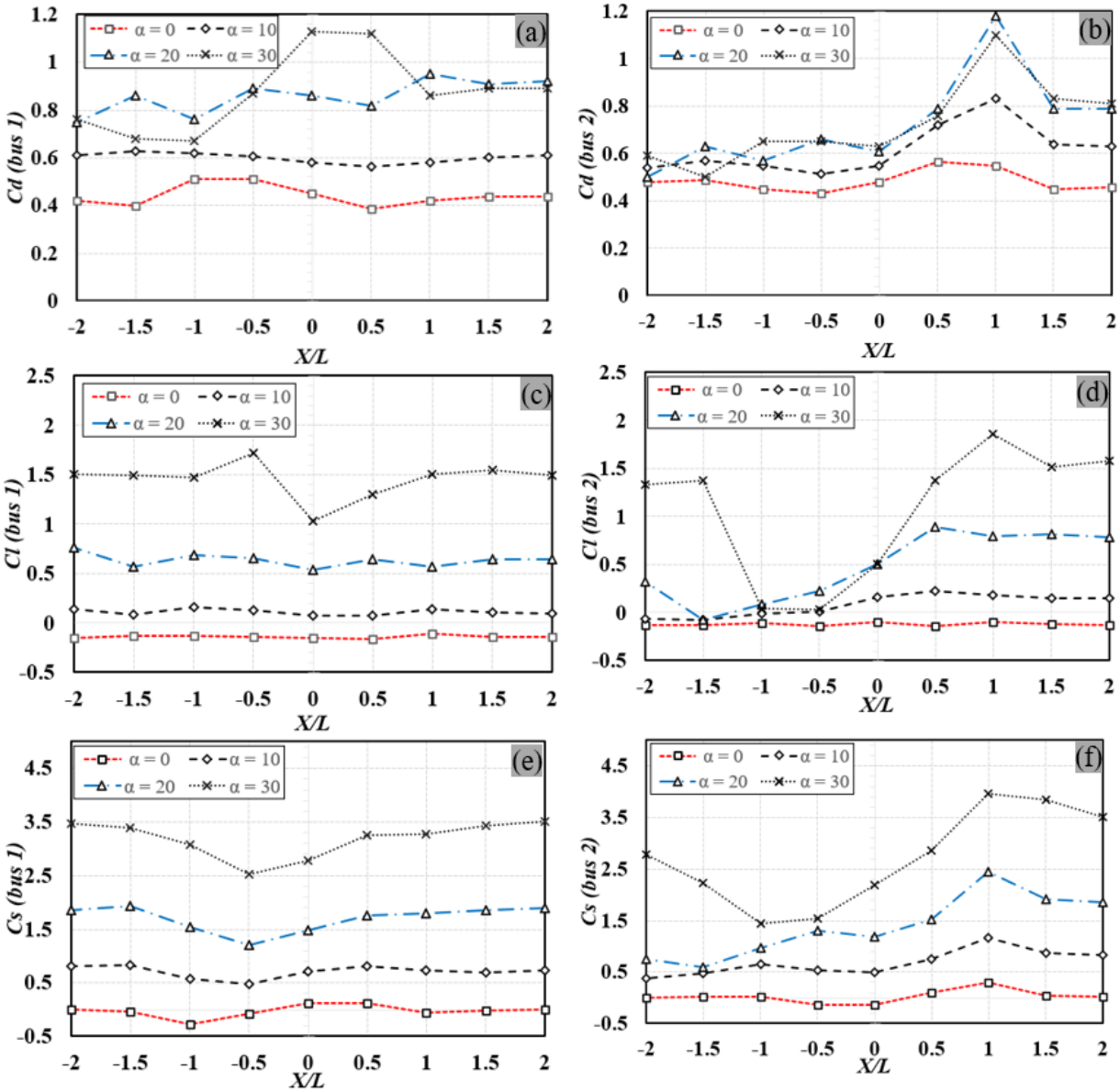

Fig. 5. Effect of X/L on the aerodynamic force coefficient of Bus1 and Bus2 at different yaw angles

The change of lift coefficient (C_L) and side force coefficient (C_s) of both buses at the yaw angle between $0°$ to $30°$ are depicted in Figure 5(c), Figure 5(d), Figure 5(e), and Figure 5(f) respectively. The value of C_L and C_s for bus1 does not change significantly during the overtaking process except when the yaw angle is $30°$. However, Bus2 experiences significant value alteration of C_L and C_s. When Bus2 is overtaking bus1 at X/L=-1 until X/L=-0.5 the value of C_L drops close to the value of lift coefficient of the bus without crosswind. A similar trend occurs on the C_s value of Bus2. When the

yaw angle direction is 30°, the value of C_s decrease from about 2.7 to 1.5 at X/L=-1 until X/L=-0.5. It is then increased to the value of about 4.0 at X/L=1. This can be generally said that the increment of yaw angle increases the value of all aerodynamic coefficients for both busses yet having less significant alteration for Bus1. However, the variation of aerodynamic coefficient differs significantly for Bus2 and results in the peak when Bus2 is overtaking Bus1 at X/L=1.

3.2 Turbulence Kinetic Energy with α=0 and α=30

Figure 6 depicts the energy produced by air turbulence when Bus2 is overtaking Bus1 with the absence of crosswind. A relatively high value of turbulence kinetic energy occurs unpredictably for two buses. The turbulence kinetic energy is observed through a middle horizontal plane of the bus model. When the X/L=-1.5, quite high turbulence is observed on the left side of Bus2, then the significant turbulence shifts to the right side of Bus2 when X/L=-0.5.

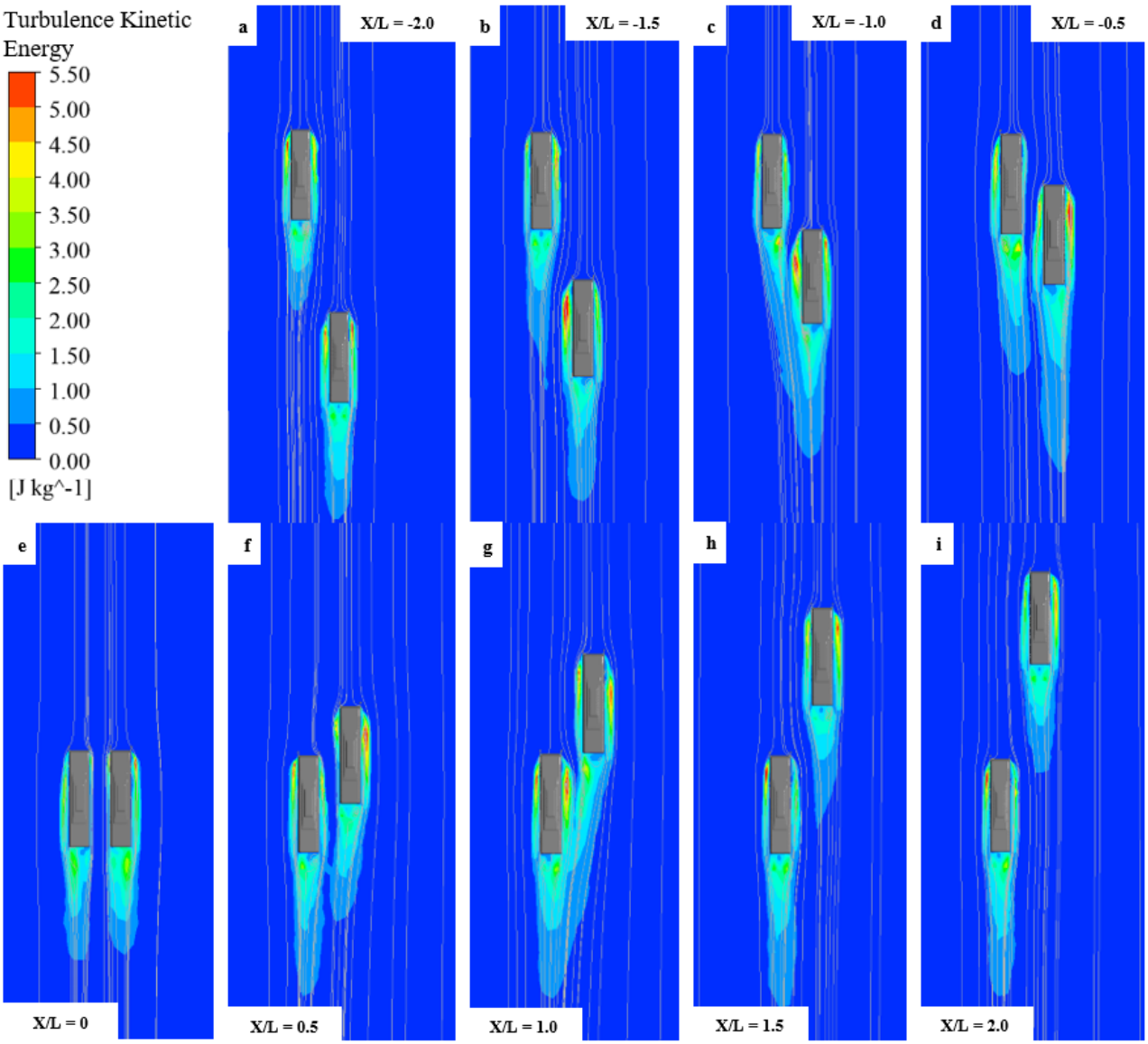

Fig. 6. Turbulence kinetic energy during overtaking without crosswind

The value is not significant when two buses are in the same row. It is followed by a higher value on both the right side of Bus2 and the left side of Bus1 when X/L=1.0. Then the kinetic energy is

getting lower towards X/L=2.0. Another point to be noted is that, when X/L equals -1.0 and 1.0, the tail of turbulence seems to merge. The separation of turbulence kinetic energy area then started to separate at X/L=-0.5 and X/L=1.5.

The most severe condition when the crosswind produces $30°$ of yaw angle is shown in Figure 7. The air stream from the leeward side generates a much more significant effect on the turbulence kinetic energy during the overtaking process. Since the air flows over the bus that is not in the same direction as the bus motion, a wider area generation of turbulence kinetic energy is observed. This area is the generation of wake due to the airflow through the bus that depends on the vehicle's profile and generally becomes larger as the yaw angle increases [30-33]. When X/L=-2.0, both buses experience a high turbulence kinetic energy on the right side of the bus. As Bus2 is approaching Bus1 both generated turbulence merges altogether and produces a higher turbulence area. When two buses are in the same row, Bus1 does not generate turbulence as much as Bus2. However, when X/L=0.5 Bus1 produces the highest value of turbulence kinetic energy over every position in the overtaking process at the right side of the bus. Since then, the turbulence kinetic energy area is getting separated until Bus1 is completely overtaken by Bus2.

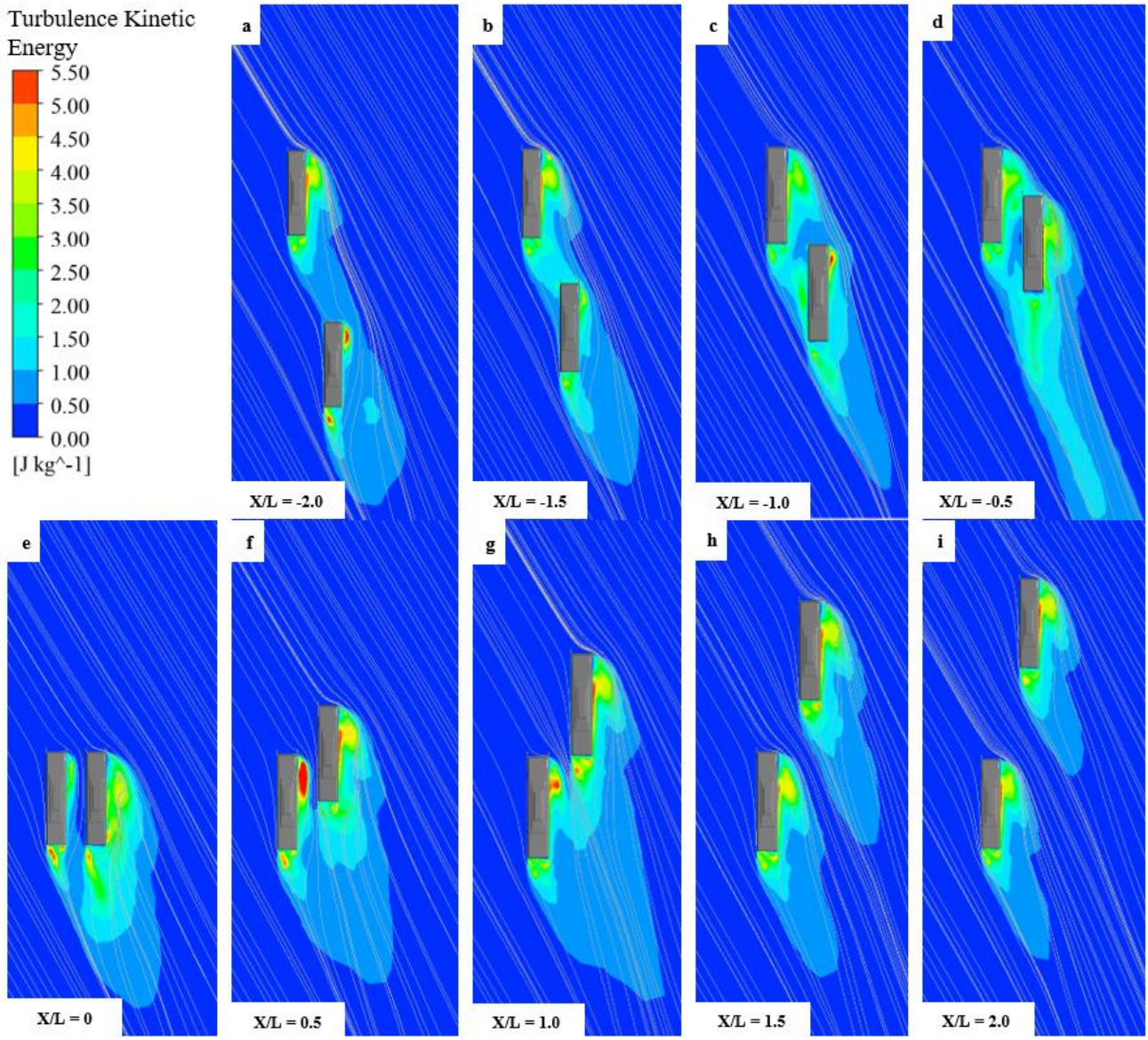

Fig. 7. Turbulence kinetic energy during overtaking at α=30

3.3 Pressure Coefficient at X/L=1

It has been mentioned in the previous section that the most prominent alteration value of the aerodynamic coefficient occurs when X/L=1. Figure 8 portrays the pressure coefficient at the bus surfaces and Figure 9 depicts the results of the pressure coefficient at the area around the vehicle at different yaw angle conditions. A positive value of the pressure coefficient can be observed at the front part of the bus when the crosswind is absent. A wide area of the front shield produces the highest positive result in pressure coefficient. However, the increasing value of the yaw angle causes the positive value of the pressure coefficient to shift at the front left part of the bus as depicted in Figure 8. The results of the pressure coefficient area can also be identified on the area around the bus as shown in Figure 9. The positive value of the pressure coefficient occurs on the front part of the bus and is getting shifted to the left side of the bus as the yaw angle elevates. The more yaw angle applied, the results of negative pressure coefficient shift to the left side of the bus. It can be noticed that the negative value of the pressure coefficient occurs at the whirlpool of the streamline of the wind.

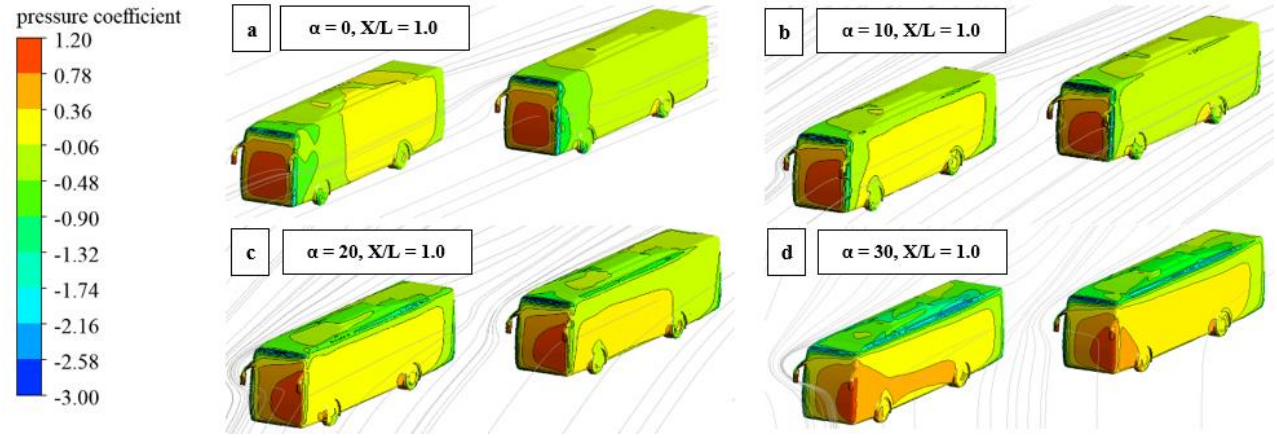

Fig. 8. Pressure coefficient at the bus surface at different yaw angles

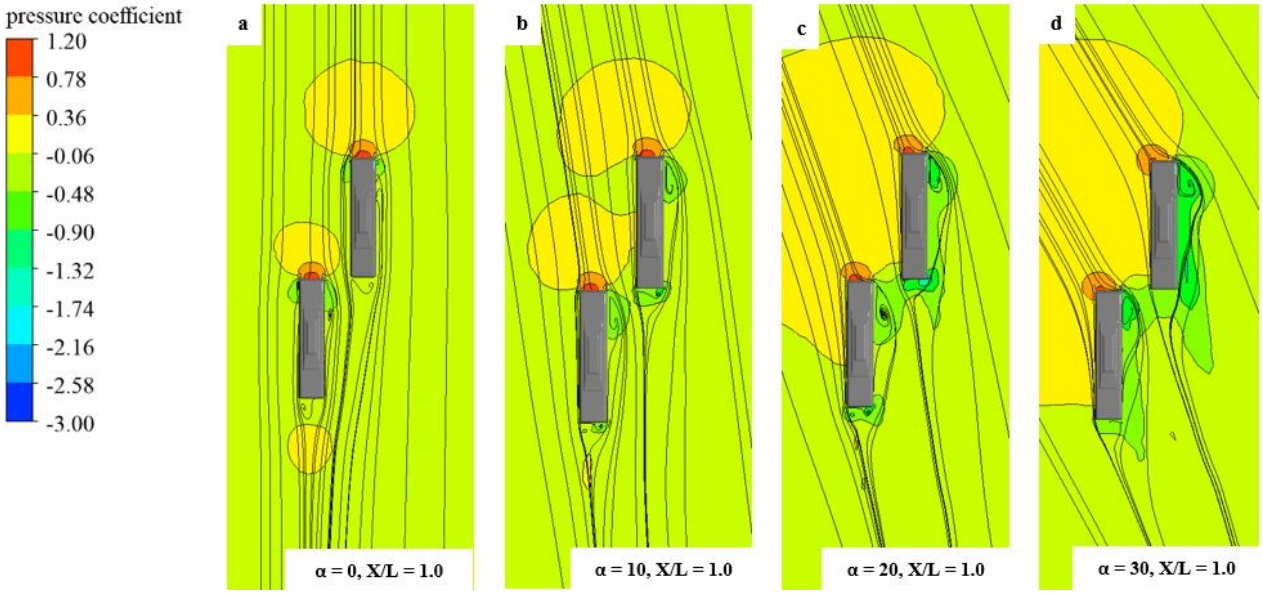

Fig. 9. Pressure coefficient around the vehicle at different yaw angles

4. Results Validation

The accuracy of the calculation of the numerical results needs to be verified. The numerical results validation utilized the comparison between the simulation resulting from the Ahmed body shape and the data obtained through the experiment by Meile *et al.,* [34]. The results on drag coefficient (C_D) and lift coefficient (C_L) were observed and compared between simulation and experiment. It can be observed that the results of simulation were generally consistent compared to the experimental testing. The different percentage of drag coefficient was about 0.37% and the lift coefficient was 2.90%. Therefore, the simulation results in this study are generally represent the value of the real testing.

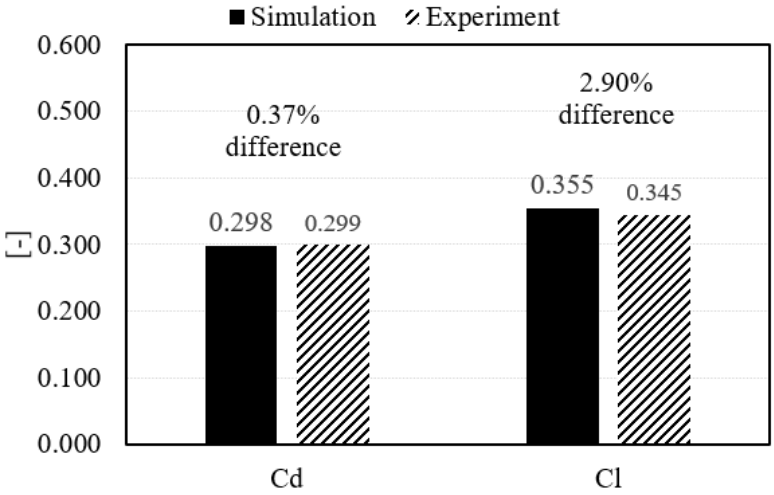

Fig. 10. Percentage of difference between the simulation and experimental validation

5. Conclusion

The overtaking process of a scaled bus model under crosswind was numerically investigated in a simulation in this study. The aerodynamic coefficient of the bus model changed significantly at the position of X/L=1 as compared to other positions. The presents of crosswind resulted in a higher value of the aerodynamic coefficient for each bus model. The examination in the turbulence kinetic energy showed that a significant increase of turbulence kinetic energy occurred for higher yaw angles particularly at X/L=0.5 and XL=1. In terms of pressure coefficient, the positive value area became larger as the yaw angle increase giving more whirlpool at the leeward side of the bus. The planned case for further study is to experimentally investigate the influence of the main part of the bus model to study the resulting behavior of the whirlpool around the bus and to increase the aerodynamic performance of the proposed bus model.

Acknowledgement
This work was fully funded by RG Auto-Body Research Fund [SP-DIPA-023.17.2.677509/2021], supported by Automotive Design Laboratory and CADD Laboratory *Universitas Negeri Yogyakarta* for the licensed software.

References

[1] Sun, Hao, Evangelos Karadimitriou, Xue Min Li, and Dimitrios Mathioulakis. "Aerodynamic Interference between Two road vehicle models during overtaking." *Journal of Energy Engineering* 145, no. 2 (2019): 04019002.

https://doi.org/10.1061/(ASCE)EY.1943-7897.0000601
[2] Cheng, S. Y., Makoto Tsubokura, Takuji Nakashima, Takahide Nouzawa, and Yoshihiro Okada. "A numerical analysis of transient flow past road vehicles subjected to pitching oscillation." *Journal of Wind Engineering and Industrial Aerodynamics* 99, no. 5 (2011): 511-522. https://doi.org/10.1016/j.jweia.2011.02.001
[3] Brandt, Adam, Bengt Jacobson, and Simone Sebben. "High speed driving stability of road vehicles under crosswinds: an aerodynamic and vehicle dynamic parametric sensitivity analysis." *Vehicle System Dynamics* (2021): 1-24. https://doi.org/10.1080/00423114.2021.1903516
[4] Yudianto, A., Saeid Ghafari, Pierre Huet, and Muhkamad Wakid. "Evaluation of the Temperature Distribution and Structural Deformation of the Car Dashboard Subjected to Direct Sunlight." In *Journal of Physics: Conference Series*, vol. 1273, no. 1, p. 012076. IOP Publishing, 2019. https://doi.org/10.1088/1742-6596/1273/1/012076
[5] Ibrahim, Nurru Anida, Idrus Salimi Ismail, Siti Norbakyah Jabar, and Salisa Abdul Rahman. "A Study on the Effects of Plug-In Hybrid Electric Vehicle (PHEV) Powertrain on Fuel Consumption, Electric Consumption and Emission using Autonomie." *Journal of Advanced Research in Applied Sciences and Engineering Technology* 16, no. 1 (2019): 49-56.
[6] Shaharuddin, Nur Haziqah, Mohamed Sukri Mat Ali, Shuhaimi Mansor, Sallehuddin Muhamad, Sheikh Ahmad Zaki Shaikh Salim, and Muhammad Usman. "Flow simulations of generic vehicle model SAE type 4 and DrivAer Fastback using OpenFOAM." *Journal of Advanced Research in Fluid Mechanics and Thermal Sciences* 37, no. 1 (2017): 18-31.
[7] Huang, Taiming, Zhengqi Gu, Chengjie Feng, and Wei Zeng. "Transient aerodynamics simulations of a road vehicle in the crosswind condition coupled with the vehicle's motion." *Proceedings of the Institution of Mechanical Engineers, Part D: Journal of Automobile Engineering* 232, no. 5 (2018): 583-598. https://doi.org/10.1177/0954407017704609
[8] Howell, Jeff, Kevin Garry, and Jenny Holt. "The aerodynamics of a small car overtaking a truck." *SAE International Journal of Passenger Cars-Mechanical Systems* 7, no. 2014-01-0604 (2014): 626-638. https://doi.org/10.4271/2014-01-0604
[9] Lazăr, Sergiu. "Computerized dynamic fluid simulation (CFD) for measuring the influence of the cab deflector on the aerodynamics of trucks." *Journal of Research and Innovation for Sustainable Society* 3, no. 1 (2021): 11-17. https://doi.org/10.33727/JRISS.2021.1.2:11-17
[10] Anwar, Faisal, Rohan Arun Gulavani, Sujit Chalipat, and Satish Jadhav. *Aero Drag Improvement Study on Large Commercial Vehicles Using CFD Lead Approach*. No. 2021-26-0424. SAE Technical Paper, 2021. https://doi.org/10.4271/2021-26-0424
[11] Arteaga, Oscar, Morales V. Hernán, Héctor Terán, Sonia Chacon, Mario A. Lara, Juan Rocha-Hoyos, and Ronny P. Aguirre. "Aerodynamic optimization of the body of a bus." In *IOP Conference Series: Materials Science and Engineering*, vol. 872, no. 1, p. 012002. IOP Publishing, 2020. https://doi.org/10.1088/1757-899X/872/1/012002
[12] Qi, Xiao-Ni, Yong-Qi Liu, and Guang-Sheng Du. "Experimental and numerical studies of aerodynamic performance of trucks." *Journal of Hydrodynamics, Ser. B* 23, no. 6 (2011): 752-758. https://doi.org/10.1016/S1001-6058(10)60173-4
[13] Buscariolo, Filipe Fabian, Felipe Magazoni, Leonardo José Della Volpe, Flavio Koiti Maruyama, and Julio Cesar Lelis Alves. *Truck Trailer Aerodynamic Design Optimization Through CFD Simulations*. No. 2019-36-0103. SAE Technical Paper, 2020. https://doi.org/10.4271/2019-36-0103
[14] Bayındırlı, Cihan, Yahya Erkan Akansu, and Mustafa Sahir Salman. "The determination of aerodynamic drag coefficient of truck and trailer model by wind tunnel tests." *International Journal of Automotive Engineering and Technologies* 5, no. 2 (2016): 53-60. https://doi.org/10.18245/ijaet.11754
[15] Zhang, Qianwen, Chuqi Su, Yi Zhou, Chengcai Zhang, Jiuyang Ding, and Yiping Wang. "Numerical investigation on handling stability of a heavy tractor semi-trailer under crosswind." *Applied Sciences* 10, no. 11 (2020): 3672. https://doi.org/10.3390/app10113672
[16] Hemida, Hassan, and Siniša Krajnović. "Transient simulation of the aerodynamic response of a double-deck bus in gusty winds." *Journal of Fluids Engineering* 131, no. 3 (2009): 031101. https://doi.org/10.1115/1.3054288
[17] Xiang, Huoyue, Yongle Li, Suren Chen, and Cuijuan Li. "A wind tunnel test method on aerodynamic characteristics of moving vehicles under crosswinds." *Journal of Wind Engineering and Industrial Aerodynamics* 163 (2017): 15-23. https://doi.org/10.1016/j.jweia.2017.01.013
[18] Yudianto, Aan, I. Wayan Adiyasa, and Afri Yudantoko. "Aerodynamics of Bus Platooning under Crosswind." *Automotive Experiences* 4, no. 3 (2021): 119-130.
[19] Kim, Se-Jin, Chul-Hwan Yoo, and Ho-Kyung Kim. "Vulnerability assessment for the hazards of crosswinds when vehicles cross a bridge deck." *Journal of Wind Engineering and Industrial Aerodynamics* 156 (2016): 62-71. https://doi.org/10.1016/j.jweia.2016.07.005
[20] Yudianto, A., H. Tan, Z. Qu, Q. Xue, A. C. Naveen, M. Mushtaq, and K. S. Gopi. "Feasibility study of a facility to produce injection molded parts for automotive industry." *International Journal of Production Management and*

Engineering 8, no. 1 (2020): 45-57. https://doi.org/10.4995/ijpme.2020.12360
[21] Dorigatti, F., M. Sterling, C. J. Baker, and A. D. Quinn. "Crosswind effects on the stability of a model passenger train-A comparison of static and moving experiments." *Journal of Wind Engineering and Industrial Aerodynamics* 138 (2015): 36-51. https://doi.org/10.1016/j.jweia.2014.11.009
[22] Quazi, Ariq, Timothy Crouch, James Bell, Tony McGreevy, Mark C. Thompson, and David Burton. "A field study on the aerodynamics of freight trains." *Journal of Wind Engineering and Industrial Aerodynamics* 209 (2021): 104463. https://doi.org/10.1016/j.jweia.2020.104463
[23] Dong, Tianyun, Guglielmo Minelli, Jiabin Wang, Xifeng Liang, and Sinisa Krajnović. "The effect of ground clearance on the aerodynamics of a generic high-speed train." *Journal of Fluids and Structures* 95 (2020): 102990. https://doi.org/10.1016/j.jfluidstructs.2020.102990
[24] Liu, Li-Ning, Xue-Feng Chi, Guang-Sheng Du, and Li Lei. "Aerodynamic characteristics of vans during accelerated overtaking process in crosswinds." *Journal of ZheJiang University (Engineering Science)* 53, no. 1 (2019): 174-179.
[25] Llorca, Carlos, Antonio Angel-Domenech, Fernando Agustin-Gomez, and Alfredo Garcia. "Motor vehicles overtaking cyclists on two-lane rural roads: Analysis on speed and lateral clearance." *Safety Science* 92 (2017): 302-310. https://doi.org/10.1016/j.ssci.2015.11.005
[26] Niknahad, Ali, and Abdolamir Bak Khoshnevis. "Numerical study and comparison of turbulent parameters of simple, triangular, and circular vortex generators equipped airfoil model." *Journal of Advanced Research in Numerical Heat Transfer* 8, no. 1 (2022): 1-18.
[27] Liu, Lining, Yumei Sun, Xuefeng Chi, Guangsheng Du, and Meng Wang. "Transient aerodynamic characteristics of vans overtaking in crosswinds." *Journal of Wind Engineering and Industrial Aerodynamics* 170 (2017): 46-55. https://doi.org/10.1016/j.jweia.2017.07.014
[28] Su, Chuqi, Zhen Hu, Qianwen Zhang, Xiaohong Yuan, Chengcai Zhang, and Yiping Wang. "Coupling analysis of transient aerodynamic and dynamic response of cars in overtaking under crosswinds." *Engineering Applications of Computational Fluid Mechanics* 14, no. 1 (2020): 1215-1227. https://doi.org/10.1080/19942060.2020.1803970
[29] Suzuki, Minoru, Katsuji Tanemoto, and Tatsuo Maeda. "Aerodynamic characteristics of train/vehicles under cross winds." *Journal of Wind Engineering and Industrial Aerodynamics* 91, no. 1-2 (2003): 209-218. https://doi.org/10.1016/S0167-6105(02)00346-X
[30] McArthur, Damien, David Burton, Mark Thompson, and John Sheridan. "An experimental characterisation of the wake of a detailed heavy vehicle in cross-wind." *Journal of Wind Engineering and Industrial Aerodynamics* 175 (2018): 364-375. https://doi.org/10.1016/j.jweia.2018.01.033
[31] Kamal, Muhammad Nabil Farhan, Izuan Amin Ishak, Nofrizalidris Darlis, Daniel Syafiq Baharol Maji, Safra Liyana Sukiman, Razlin Abd Rashid, and Muhamad Asri Azizul. "A Review of Aerodynamics Influence on Various Car Model Geometry through CFD Techniques." *Journal of Advanced Research in Fluid Mechanics and Thermal Sciences* 88, no. 1 (2021): 109-125. https://doi.org/10.37934/arfmts.88.1.109125
[32] Wieser, Dirk, Christian Navid Nayeri, and Christian Oliver Paschereit. "Wake structures and surface patterns of the drivaer notchback car model under side wind conditions." *Energies* 13, no. 2 (2020): 320. https://doi.org/10.3390/en13020320
[33] Yudianto, A., H. A. Susanto, A. Suyanto, I. W. Adiyasa, A. Yudantoko, and N. A. Fauzi. "Aerodynamic performance analysis of open-wheel vehicle: Investigation of wings installation under different speeds." In *Journal of Physics: Conference Series*, vol. 1700, no. 1, p. 012086. IOP Publishing, 2020. https://doi.org/10.1088/1742-6596/1700/1/012086
[34] Meile, Walter, Günter Brenn, Aaron Reppenhagen, Bernhard Lechner, and Anton Fuchs. "Experiments and numerical simulations on the aerodynamics of the Ahmed body." *CFD Letters* 3, no. 1 (2011): 32-39.